Universal exotic dynamics in critical mesoscopic systems: Simulating the square root of Avogadro's number of spins

Mauro Bisson [1,*] Alexandros Vasilopoulos [2,*] Massimo Bernaschi,[3] Massimiliano Fatica [1] Nikolaos G. Fytas [2,†] Isidoro González-Adalid Pemartín [3] and Víctor Martín-Mayor [4]

[1]*NVIDIA Corporation, Santa Clara, California 95051, USA*

[2]*School of Mathematics, Statistics and Actuarial Science, University of Essex, Colchester CO4 3SQ, United Kingdom*

[3]*Istituto per le Applicazioni del Calcolo, CNR, Via dei Taurini 19, 00185 Rome, Italy*

[4]*Departamento de Física Téorica I, Universidad Complutense, 28040 Madrid, Spain*

(Received 17 March 2025; accepted 29 July 2025; published 4 September 2025)

We explicitly demonstrate the universality of critical dynamics through unprecedented large-scale Graphics Processing Units (GPU)-based simulations of two out-of-equilibrium processes, comparing the behavior of spin-1/2 Ising and spin-1 Blume-Capel models on a square lattice. In the first protocol, a completely disordered system is instantaneously brought into contact with a thermal bath at the critical temperature, allowing it to evolve until the coherence length exceeds 10^3 lattice spacings. Finite-size effects are negligible due to the mesoscopic scale of the lattice sizes studied, with linear dimensions up to $L = 2^{22}$ and 2^{19} for the Ising and Blume-Capel models, respectively. Our numerical data, and the subsequent analysis, demonstrate a strong dynamic universality between the two models and provide the most precise estimate to date of the dynamic critical exponent for this universality class, $z = 2.1676(1)$. In the second protocol, we corroborate the role of the universal ratio of dynamic and static length scales in achieving an exponential acceleration in the approach to equilibrium just *above* the critical temperature, through a time-dependent variation of the thermal bath temperature. The results presented in this work leverage our Compute Unified Device Architecture (CUDA)-based numerical code, breaking the world record for the simulation speed of the Ising model.

DOI: 10.1103/ngkf-7816

I. INTRODUCTION

Counterintuitive phenomena emerge when a system attempts to reach thermal equilibrium following a temperature change. Examples include remarkable memory and rejuvenation effects in spin glasses [1–3], as well as the Mpemba effect, in which, under certain conditions, the hotter of two identical beakers of water cools faster when placed in contact with a thermal reservoir colder than both [4–7] and its variants (see, e.g., Refs. [8–10]). Theoretical analysis is often limited to systems in which the contribution of a single timescale is manipulated by varying the temperature of the external bath, leading to surprising effects [11–13]. However, similar phenomena also occur when a continuum of timescales is relevant, such as near a second-order phase transition [14] or deep inside the spin-glass phase [1,15]. It is hoped that universality—the insensitivity of macroscopic behavior to microscopic details [16]—may aid the analysis of problems governed by multiple timescales.

The concepts of critical phenomena can, fortunately, be extended to dynamical processes (see Ref. [17] for a seminal review). However, while universality is well established for equilibrium properties, its extension to dynamical properties remains less clear and lags behind its theoretical counterpart [17,18]. A rigorous solution to the critical dynamics of the simplest fruit-fly model in statistical physics—the two-dimensional Ising model [19–21]—remains elusive. Moreover, models within the same static universality class do not necessarily belong to the same dynamic universality class [22]. In fact, the discussion becomes even more complex for disordered systems [23], where violations of universality have been reported [24,25].

A particularly fundamental and nontrivial case arises in models whose equilibrium critical properties belong to the same universality class as the Ising ferromagnet. A representative example is the spin-1 Blume-Capel model [26,27], specifically in its second-order transition regime [28]. As is well known, the onset of criticality is marked by a divergence of both the correlation length ξ and the correlation time τ. While the former divergence yields singularities in static quantities, the latter manifests notably as critical slowing down. To describe dynamical scaling properties, an additional exponent is required in addition to the static exponents. This so-called dynamic critical exponent z links the divergence of length and timescales, i.e., $\tau \sim \xi_{\rm eq}^z$ [29–32] ($\xi_{\rm eq}$ is the correlation length in equilibrium). In a finite system, $\xi_{\rm eq}$ is bounded by the linear system size L, so that $\tau \sim L^z$ at the incipient

*These authors contributed equally to this work.
†Contact author: nikolaos.fytas@essex.ac.uk

critical point. The dynamic critical exponent z has been numerically determined to be $z = 2.1665(12)$ in two dimensions in the seminal work by Nightingale and Blöte [29], and was later shown to be universal with respect to the underlying lattice structure [33]. The more recent theoretical studies based on the nonperturbative renormalization-group [34] and the ε-expansion [35], suggesting $z \approx 2.15$ and 2.14(2), respectively, should also be noted.

However, even the simplest equilibration protocol—where the system is instantaneously quenched from a high temperature to the working temperature T, and then allowed to relax for a time t—can lead to a range of different outcomes depending on L and t. Indeed, the computation of z in Ref. [29] relies on an assumption that is well founded for finite systems (see, e.g., Refs. [36,37]), namely, a timescale τ exists such that *all* observables approach their equilibrium value when $t \approx \tau \propto L^z$. However, in the critical dynamics of a system with $L = \infty$, perfectly reasonable quantities may remain far from their equilibrium values even when $t \gg \tau$ [38,39]. Moreover, there are both experimental (see, e.g., Ref. [3]) and theoretical [40] settings in which equilibrium is never fully achieved. In these cases, the size of magnetic domains, $\xi(t)$, grows indefinitely provided $L = \infty$ and $T \leqslant T_c$, where T_c denotes the critical temperature. Precisely at $T = T_c$, one has $\xi(t) \propto t^{1/z}$, while $\xi(t) \propto \sqrt{t}$ for $T < T_c$ (if T is very close to T_c, a crossover occurs from critical dynamics at short times to $\xi(t) \propto \sqrt{t}$ at long times). The domain growth may also persist for a long time if $T \gtrsim T_c$, in which case $\xi(t)$ must grow until it reaches its equilibrium value $\xi_{eq}(T) \propto (T/T_c - 1)^{-\nu}$ ($\nu = 1$ for the two-dimensional Ising universality class). It is generally expected that the domain-growth exponent z in this context matches the exponent z observed in the equilibrium, finite-size setting; however, precision tests to confirm this expectation are currently lacking.

In this article, we demonstrate that universality holds for the critical dynamics of two ferromagnetic models belonging to the same *static* universality class: the spin-1/2 Ising ferromagnet and the spin-1 Blume-Capel model, within the $L \gg \xi(t)$ regime. The largest simulated system contains $2^{44} \approx 17.6 \times 10^{12}$ spins, which is more than the square root of Avogadro's number of spins. Thus, even though we reach $\xi(t)$ values well above 10^3 lattice spacings, our simulations fully represent the thermodynamic limit. In this way, we provide the most accurate determination to date of the exponent z, which turns out to be compatible with, but more precise than, the best estimate in the thermal equilibrium regime (i.e., $\xi(t) \gg L$) [29]. We showcase universality not only in the direct-quench settings discussed above, but also in the exponential speedup achieved through precooling [14]. Our results were made possible by a CUDA program that has been made publicly available elsewhere [41] for multi GPU-based simulations, which is an extension of Ref. [42], setting a world record for the simulation speed of the square-lattice Ising model, achieving 8.7 fs per spin update. The code implements the Metropolis algorithm and exploits three levels of parallelism: multispin coding, checkerboard decomposition, and domain decomposition. From this viewpoint, the current work represents the dawn of an upcomming era in computational statistical physics of lattice spin models.

II. MODELS AND PHYSICAL OBSERVABLES

The Blume-Capel (BC) ferromagnet is described by the Hamiltonian

$$\mathcal{H}^{(\mathrm{BC})} = -J \sum_{\langle \mathbf{x},\mathbf{y} \rangle} \sigma_{\mathbf{x}} \sigma_{\mathbf{y}} + \Delta \sum_{\mathbf{x}} \sigma_{\mathbf{x}}^2, \tag{1}$$

where the spins $\sigma_{\mathbf{x}} = \{-1, 0, +1\}$ are located in the nodes of an $L \times L$ square lattice with periodic boundary conditions, $\langle \mathbf{x}, \mathbf{y} \rangle$ indicates summation over nearest neighbors, and $J > 0$ is the ferromagnetic exchange coupling. The parameter Δ is known as the crystal-field coupling that controls the density of vacancies ($\sigma_{\mathbf{x}} = 0$). For $\Delta \to -\infty$, vacancies are suppressed and the model becomes equivalent to the simple Ising ($\sigma_{\mathbf{x}} = \pm 1$) ferromagnet. The phase boundary of the Blume-Capel model in the crystal field-temperature plane separates the ferromagnetic from the paramagnetic phase [28]. At high temperatures and low crystal fields, the ferromagnetic-paramagnetic transition is a continuous phase transition in the Ising universality class, whereas at low temperatures and high crystal fields, the transition is of first order [26,27]. At zero temperature, the ferromagnetic order prevails and the point ($\Delta_0 = n_c J/2, T = 0$), where n_c denotes the coordination number, lies on the phase boundary [27]. On the other hand, for zero crystal field, the transition temperature is not exactly known. For the present square-lattice model under study, we provide a high-accuracy estimate $T_c^{(\mathrm{BC})}(\Delta = 0) = 1.693\,5583(5)$ [43]. This result was obtained through a dedicated finite-size scaling analysis, which combines exact results for this universality class [44–47] with extensive Swendsen-Wang simulations [48] on systems with linear sizes up to $L \leqslant 4096$. For comparison, in the case of the simple Ising model (IM), the exact critical temperature used in the simulations below is $T_c^{(\mathrm{IM})} = 2/\log(1 + \sqrt{2})$.

The main quantities of interest are the correlation function

$$C(\mathbf{r}; t) = \frac{1}{L^2} \sum_{\mathbf{x}-\mathbf{y}=\mathbf{r}} \langle \sigma_{\mathbf{x}}(t) \sigma_{\mathbf{y}}(t) \rangle \tag{2}$$

and the energy density

$$E(t) = C[\mathbf{r} = (1, 0); t] + C[\mathbf{r} = (0, 1); t], \tag{3}$$

where $\langle \cdots \rangle$ stands for the average over independent realizations of our thermal protocols, and periodic boundary conditions are understood. We extract the coherence length $\xi(t)$ from space integrals of $C(\mathbf{r}; t)$, as explained in Refs. [14,49,50]. Interestingly enough, the long- and short-distance behavior of $C(\mathbf{r}; t)$ at T_c is related through the energy's scaling dimension [51], which in our case is $D - 1/\nu = 1$. Hence [52,53], at T_c, the energy excess

$$E(t) - E_{eq} \propto [\xi(T_c, t)]^{-(D-1/\nu)} \propto t^{-(1/z)}, \tag{4}$$

where E_{eq} denotes its equilibrium value, provides a short-distance estimate of the dynamic critical exponent z. For full details of our simulations and analysis methods, we refer the reader to Ref. [43].

III. THERMAL PROTOCOLS

We consider two different thermal protocols. In the direct quench, the system is instantaneously brought from $T = \infty$

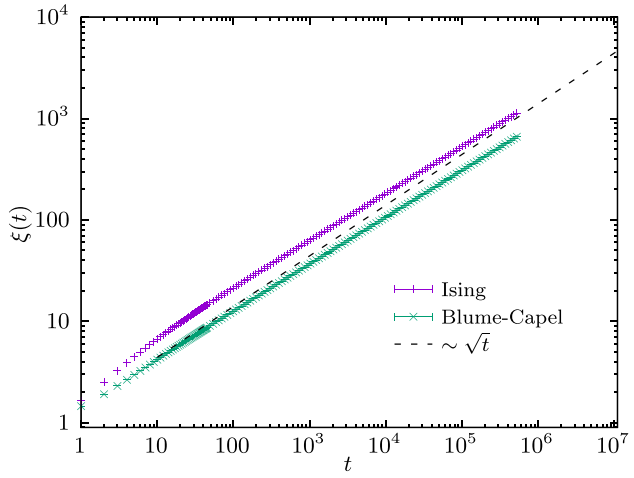

FIG. 1. Coherence length ξ as a function of time t for both the Ising ($L = 2^{22}$) and Blume-Capel ($L = 2^{19}$) models at their respective critical points.

(i.e., a fully disordered configuration) to the working temperature T where it is left to relax while the coherence length $\xi(t)$ grows (see Figs. 1 and 2). The second protocol is a precooling strategy, where a fully disordered configuration is initially placed at a temperature $T_1 \approx 0.73T_c$, allowed to relax for some time, and then heated to a higher temperature $T_2 \gtrsim T_c$, where it reaches equilibrium. This protocol is characterized by the fraction f of the equilibrium coherence length $\xi_{eq}(T_2)$ that the system reaches while evolving at the lower temperature T_1 just before the change to temperature T_2, as shown in Fig. 2. In Ref. [14] an exponential dynamic speedup was observed for the Ising model with $\xi_{eq}(T_2) \leqslant 135$, provided that $f = 0.59(7)$. It was speculated that this speedup is universal.

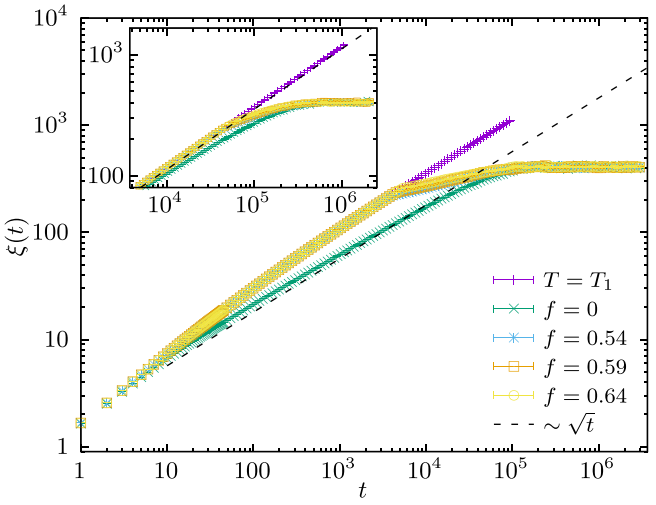

FIG. 2. Coherence length ξ for a linear size $L = 2^{16}$ as a function of time t for both the Ising (main panel) and Blume-Capel (inset) models, following the second thermal protocol. $\xi(t)$ appears to be almost f-independent in this case.

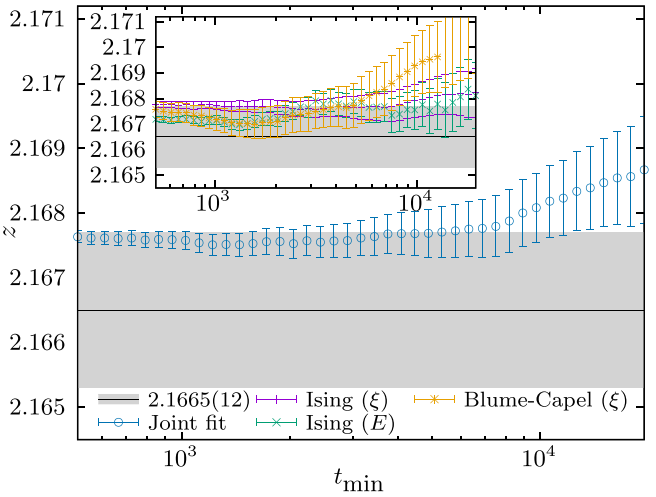

FIG. 3. Estimates of the dynamic critical exponent z for the Ising ($L = 2^{22}$) and Blume-Capel ($L = 2^{19}$) models obtained via nonlocal [ξ, Eq. (5)] and local [E, Eq. (6)] observables, for a varying fitting window (t_{min}: shortest time included in the fit). The main panel displays results from a joint fit for both models (considering data from ξ and E for the Ising model, and only ξ for the Blume-Capel model), as indicated in the legend. The inset shows three sets of data points corresponding to individual fits for each model. We have acceptable values of the fits' figure of merit χ^2/dof for all the t_{min} shown. In both panels, the solid line with the gray-scale background corresponds to $z = 2.1665(12)$ [29].

IV. RESULTS

We determine the dynamic critical exponent z from our direct-quench simulations for both models at their respective critical points (see Fig. 3). To validate universality, we perform fits of $\xi(t)$ of the form

$$\log(t) = z\log[\xi(t)] + b + b'\xi(t)^{-\omega}, \tag{5}$$

across the data from both models. Here, b and b' are nonuniversal fitting constants and $\omega = 1.75$ is the correction-to-scaling exponent for the Ising universality class (see, for example, the discussion in the Supplemental Material of Refs. [54,55]). Furthermore, we compute z also from the energy $E(t)$, as outlined in Eq. (4), exclusively for the Ising model, since only in this case is the equilibrium energy value exactly known [$E_{eq}(T_c) = -\sqrt{2}$]. We consider a fit of the form

$$E(t) - E_{eq} = bt^{-(1/z)} + b't^{-(2/z)} + b''t^{-[(\omega+1)/z]}, \tag{6}$$

where again b, b', and b'' are nonuniversal fitting constants. Indeed, for a system of size L in *equilibrium*, one has $\langle E_L\rangle + \sqrt{2} = c_1/L + \mathcal{O}(L^{-2})$, where c_1 is a known constant [56]. Dynamic scaling asserts that we can apply the equilibrium result by replacing L with $\xi(t)$ (noting that amplitudes, such as c_1, may differ from their equilibrium values). To ensure our determination of z from the energy is independent of long-distance observables, we have further replaced $\xi(t)$ with $t^{1/z}$. Additionally, we have included a correction term, $t^{-[(\omega+1)/z]}$, to account for scaling corrections in $\xi(t)$, as described in Eq. (5) that we have inverted as $\xi = B_0 t^{1/z}(1 + B_1/t^{\omega/z} + \cdots)$, where B_0 and B_1 are scaling amplitudes.

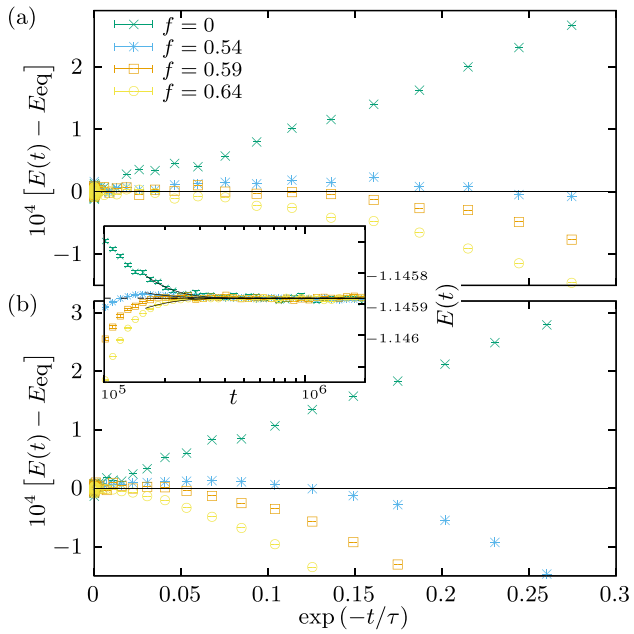

FIG. 4. Energy's convergence to its equilibrium value ($E_{\rm eq}$) within the two-step thermal protocol scheme for the (a) Ising and (b) Blume-Capel models. We recall that, for the case of the Ising ferromagnet, $E_{\rm eq}$ is known exactly from the Onsager solution. The inset highlights $E(t)$ in the large-time window for the Blume-Capel case. Results for $L = 2^{16}$ are shown.

Our fitting results are documented in Fig. 3. In particular, the main panel presents the dynamic exponent z, which we obtained from a joint fit across three datasets, as indicated in the legend. The estimates for z fall within the range 2.167 63(9)–2.1678(5) and we report the final result as

$$z = 2.1676(1), \tag{7}$$

which corresponds to the logarithmic midpoint of the stable region shown in the main plot. This value is in excellent agreement with the result of $z = 2.1665(12)$ reported by Nightingale and Blöte [29]. Notably, the error in our calculation is approximately one-twelfth of the error reported in Ref. [29]. In the inset of Fig. 3, we show the individual z estimates obtained from separate fits to each of the three datasets, which further support the validity of both the joint fit and the result in Eq. (7). For more details about the fits and our statistical accuracy criteria, we refer to [43]. Note also that the absence of finite-size effects for $\xi(t)$ and $E(t)$ (within our time window and statistical errors) was assessed by comparing results for the Ising model on systems with $L = 2^{20}$ and 2^{22} linear dimensions (see Ref. [43] for details).

Next, we focus on the approach to equilibrium in the paramagnetic phase for $T_2 \gtrsim T_c$. Specifically, we choose T_2, such that the equilibrium values of ξ are $\xi_{\rm eq}(T_2) = 407(1)$ for the Ising model and 405(2) for the Blume-Capel model. We then examine the approach to equilibrium of the energy under different thermal protocols, as shown in Fig. 4. The different protocols maintain $T_1 \approx 0.73T_c$ until $\xi(t, T1) = f\xi_{\rm eq}(T_2)$, and then the system is instantaneously placed in contact with the thermal bath at T_2. The direct quench, where $f = 0$, is shown in Fig. 4. In the case of direct quench, $E(t)$ approaches equilibrium monotonically from above, whereas the three precooling strategies begin well below the asymptotic equilibrium value. However, $E(t; f = 0.54)$ overshoots the equilibrium value of the energy and approaches equilibrium from *above*, while $E(t; f = 0.59)$ and $E(t; f = 0.64)$ approach equilibrium from *below*. An exponential law turns out to aptly fit the late approach to equilibrium

$$E(t; f) = E_{\rm eq} + b(f)\exp(-t/\tau), \tag{8}$$

where the fitting parameters for the Ising model are the amplitude $b(f)$ and the timescale τ, with $E_{\rm eq}$ known from Onsager's solution. We perform a joint fit to the data for all values of f, because τ is f-independent in Eq. (8). For the Blume-Capel model, which lacks an exact solution, we have to include $E_{\rm eq}$ as an f-independent parameter in the joint fit. In this way, we find for both models $b^{\rm IM}(f = 0.59) = 0.000\,00(2)$, $b^{\rm BC}(f = 0.59) = 0.000\,00(6)$. Furthermore, the amplitudes are positive at $f = 0.54$ [$b^{\rm IM}(f = 0.54) = 0.000\,15(3)$, $b^{\rm BC}(f = 0.54) = 0.000\,28(6)$] and negative at $f = 0.64$ [$b^{\rm IM}(f = 0.64) = -0.000\,24(4)$, $b^{\rm BC}(f = 0.64) = -0.0005(1)$]. Therefore, we propose the conservative estimate $f = 0.59(5)$ as the universal value at which the exponential speedup in the approach to equilibrium occurs in the scaling limit for both the Ising and Blume-Capel models.

V. DISCUSSION

Although there are strong theoretical reasons to expect universality in dynamical critical phenomena [16,17], high-accuracy computations confirming this are still scarce. Moreover, dynamics opens up a broader range of questions. For instance, it is not at all obvious that the limits of large system size and long times are interchangeable. The computation in Ref. [29] relies on the assumption that a timescale τ exists such that *all* physical quantities approach their large-time limits with corrections of the form $\sim e^{-t/\tau}$. This assumption holds if the limit of large times is taken *before* the thermodynamic limit [36,37], but it is simply not true when the order of limits is reversed, which is the relevant case for field-theoretical computations [34,35]. Furthermore, the temperature of the thermal bath can be varied in time in clever ways to produce counterintuitive effects (see, e.g., Refs. [4–15]). Demonstrations of universality in this broader context of time-varying temperatures are rare (if at all existing), though one might argue that memory and rejuvenation effects in spin-glasses provide another example of universality [2].

In this work, we have made progress on both fronts, thanks to massive-scale simulations on GPUs. Building on ideas presented in Refs. [42,57], we developed a CUDA code that enabled us to simulate square lattices with side lengths $L = 2^{22}$ for the Ising model and $L = 2^{19}$ for the Blume-Capel model, reaching coherence lengths well over 10^3 lattice spacings. Thus, while we are taking the limit of large times, the limit of large sizes is certainly taken *before*. Through this, we have explicitly demonstrated universality by showing that both models are governed by the same dynamic exponent z. Along the way, we have obtained the best estimate to date for the dynamic critical exponent, setting a standard for comparison with field-theoretical computations. Additionally, we considered the precooling strategy from Ref. [14], which

achieves an exponential speedup in the approach to equilibrium at temperatures $T \gtrsim T_c$ by temporarily entering the ferromagnetic phase. Both the Ising and Blume-Capel models exhibit exponential speedup when the dimensionless ratio of coherence lengths reaches a specific value, a hallmark of a *dynamic universality class*. We anticipate that the numerical approach developed in this study may be adapted to help resolve ongoing debates about the universality classes of other nonequilibrium systems, including those encountered in active matter [58].

ACKNOWLEDGMENTS

Part of the numerical calculations reported in this paper were performed at the High-Performance Computing cluster CERES of the University of Essex. This work was partially supported by MCIN/AEI/10.13039/501100011033 and by "ERDF, a way of making Europe" through Grant No. PID2022-136374NB-C21. The work of A.V. and N.G.F. was supported by the Engineering and Physical Sciences Research Council (Grant No. EP/X026116/1).

DATA AVAILABILITY

The data that support the findings of this article are not publicly available upon publication because it is not technically feasible and/or the cost of preparing, depositing, and hosting the data would be prohibitive within the terms of this research project. The data are available from the authors upon reasonable request.

[1] K. Jonason, E. Vincent, J. Hammann, J. P. Bouchaud, and P. Nordblad, Memory and chaos effects in spin glasses, Phys. Rev. Lett. **81**, 3243 (1998).
[2] M. Baity-Jesi *et al.*, Memory and rejuvenation effects in spin glasses are governed by more than one length scale, Nat. Phys. **19**, 978 (2023).
[3] I. Paga *et al.* (Janus Collaboration), Quantifying memory in spin glasses, Phys. Rev. Lett. **133**, 256704 (2024).
[4] Aristotle, *Metaphysics (English translation by W.D. Ross)* (Clarendon, Oxford, 1981).
[5] M. Jeng, The Mpemba effect: When can hot water freeze faster than cold? Am. J. Phys. **74**, 514 (2006).
[6] E. B. Mpemba and D. G. Osborne, Cool? Phys. Educ. **4**, 172 (1969).
[7] J. Bechhoefer, A. Kumar, and R. Chétrite, A fresh understanding of the Mpemba effect, Nat. Rev. Phys. **3**, 534 (2021).
[8] A. Gal and O. Raz, Precooling strategy allows exponentially faster heating, Phys. Rev. Lett. **124**, 060602 (2020).
[9] A. Lapolla and A. Godec, Faster uphill relaxation in thermodynamically equidistant temperature quenches, Phys. Rev. Lett. **125**, 110602 (2020).
[10] G. Teza, J. Bechhoefer, A. Lasanta, O. Raz, and M. Vucelja, Speedups in nonequilibrium thermal relaxation: Mpemba and related effects, arXiv:2502.01758.
[11] Z. Lu and O. Raz, Nonequilibrium thermodynamics of the Markovian Mpemba effect and its inverse, Proc. Natl. Acad. Sci. USA **114**, 5083 (2017).
[12] G. Teza, R. Yaacoby, and O. Raz, Eigenvalue crossing as a phase transition in relaxation dynamics, Phys. Rev. Lett. **130**, 207103 (2023).
[13] I. G.-A. Pemartín, E. Mompó, A. Lasanta, V. Martín-Mayor, and J. Salas, Shortcuts of freely relaxing systems using equilibrium physical observables, Phys. Rev. Lett. **132**, 117102 (2024).
[14] I. González-Adalid Pemartín, E. Mompó, A. Lasanta, V. Martín-Mayor, and J. Salas, Slow growth of magnetic domains helps fast evolution routes for out-of-equilibrium dynamics, Phys. Rev. E **104**, 044114 (2021).
[15] M. Baity-Jesi *et al.*, The Mpemba effect in spin glasses is a persistent memory effect, Proc. Natl. Acad. Sci. USA **116**, 15350 (2019).
[16] J. Zinn-Justin, *Quantum Field Theory and Critical Phenomena*, 4th ed. (Clarendon Press, Oxford, 2005).
[17] P. Hohenberg and B. Halperin, Theory of dynamic critical phenomena, Rev. Mod. Phys. **49**, 435 (1977).
[18] R. Folk and G. Moser, Critical dynamics: a field-theoretical approach, J. Phys. A: Math. Gen. **39**, R207 (2006).
[19] B. M. McCoy and T. T. Wu, *The Two Dimensional Ising Model* (Harvard University Press, Cambridge, 1973).
[20] M. E. J. Newman and G. T. Barkema, *Monte Carlo Methods in Statistical Physics* (Clarendon Press, Oxford, 1999).
[21] D. P. Landau and K. Binder, *A Guide to Monte Carlo Simulations in Statistical Physics*, 2nd ed. (Cambridge University Press, Cambridge, 2005).
[22] C. Bonati, A. Pelissetto, and E. Vicari, Critical relaxational dynamics at the continuous transitions of three-dimensional spin models with $\mathbb{z}_2$ gauge symmetry, Phys. Rev. B **111**, 115129 (2025).
[23] M. Hasenbusch, A. Pelissetto, and E. Vicari, Relaxational dynamics in 3D randomly diluted Ising models, J. Stat. Mech. (2007) P11009.
[24] L. F. da Silva, U. L. Fulco, and F. D. Nobre, The two-dimensional site-diluted Ising model: a short-time-dynamics approach, J. Phys.: Condens. Matter **21**, 346005 (2009).
[25] W. Zhong, G. T. Barkema, and D. Panja, Super slowing down in the bond-diluted Ising model, Phys. Rev. E **102**, 022132 (2020).
[26] M. Blume, Theory of the first-order magnetic phase change in UO_2, Phys. Rev. **141**, 517 (1966).
[27] H. Capel, On the possibility of first-order phase transitions in Ising systems of triplet ions with zero-field splitting, Physica **32**, 966 (1966).
[28] J. Zierenberg, N. G. Fytas, M. Weigel, W. Janke, and A. Malakis, Scaling and universality in the phase diagram of the 2D Blume-Capel model, Eur. Phys. J. Spec. Top. **226**, 789 (2017).
[29] M. Nightingale and H. Blöte, Dynamic exponent of the two-dimensional Ising model and Monte Carlo computation of the subdominant eigenvalue of the stochastic matrix, Phys. Rev. Lett. **76**, 4548 (1996).
[30] M. Nightingale and H. Blöte, Monte Carlo computation of correlation times of independent relaxation modes at criticality, Phys. Rev. B **62**, 1089 (2000).

[31] M. Hasenbusch, Dynamic critical exponent z of the three-dimensional Ising universality class: Monte Carlo simulations of the improved Blume-Capel model, Phys. Rev. E **101**, 022126 (2020).

[32] Z. Liu, E. Vatansever, G. T. Barkema, and N. G. Fytas, Critical dynamical behavior of the Ising model, Phys. Rev. E **108**, 034118 (2023).

[33] F.-G. Wang and C.-K. Hu, Universality in dynamic critical phenomena, Phys. Rev. E **56**, 2310 (1997).

[34] C. Duclut and B. Delamotte, Frequency regulators for the nonperturbative renormalization group: A general study and the model a as a benchmark, Phys. Rev. E **95**, 012107 (2017).

[35] L. Adzhemyan, D. Evdokimov, M. Hnatič, E. Ivanova, M. Kompaniets, A. Kudlis, and D. Zakharov, The dynamic critical exponent z for 2d and 3d Ising models from five-loop ϵ expansion, Phys. Lett. A **425**, 127870 (2022).

[36] D. A. Levin and Y. Peres, *Markov Chains and Mixing Times* (American Mathematical Society, Providence, USA, 2017), Vol. 107.

[37] A. D. Sokal, Monte Carlo methods in statistical mechanics: Foundations and new algorithms, in *Functional Integration: Basics and Applications (1996 Cargèse School)*, edited by C. DeWitt-Morette, P. Cartier, and A. Folacci (Plenum, New York, 1997), pp. 131–192.

[38] L. A. Fernández, E. Marinari, V. Martín-Mayor, G. Parisi, and J. Ruiz-Lorenzo, Out-of-equilibrium 2D Ising spin glass: Almost, but not quite, a free-field theory, J. Stat. Mech. (2018) 103301.

[39] L. A. Fernández, E. Marinari, V. Martín-Mayor, G. Parisi, and J. Ruiz-Lorenzo, An experiment-oriented analysis of 2D spin-glass dynamics: a twelve time-decades scaling study, J. Phys. A: Math. Theor. **52**, 224002 (2019).

[40] A. J. Bray, Theory of phase-ordering kinetics, Adv. Phys. **43**, 357 (1994).

[41] M. Bisson, M. Bernaschi, M. Fatica, N. G. Fytas, I. González-Adalid Pemartín, V. Martín-Mayor, and A. Vasilopoulos, Massive-scale simulations of 2D Ising and Blume-Capel models on rack-scale multi-GPU systems, Comput. Phys. Commun. **315**, 109690 (2025).

[42] J. Romero, M. Bisson, M. Fatica, and M. Bernaschi, High performance implementations of the 2D Ising model on GPUs, Comput. Phys. Commun. **256**, 107473 (2020).

[43] See Supplemental Material at http://link.aps.org/supplemental/10.1103/ngkf-7816 for (1) simulation details, (2) computation of the critical temperature of the $\Delta = 0$ square-lattice Blume-Capel model, (3) analysis of the correlation function, (4) outline of the fitting procedure, and (5) thermodynamic limit illustrations.

[44] P. Di Francesco, H. Saleur, and J. Zuber, Critical Ising correlation functions in the plane and on the torus, Nucl. Phys. B **290**, 527 (1987).

[45] P. Di Francesco, H. Saleur, and J. Zuber, Correlation functions of the critical Ising model on a torus, Europhys. Lett. **5**, 95 (1988).

[46] J. Salas and A. D. Sokal, Universal amplitude ratios in the critical two-dimensional Ising model on a torus, J. Stat. Phys. **98**, 551 (2000).

[47] M. Caselle, M. Hasenbusch, A. Pelissetto, and E. Vicari, Irrelevant operators in the two-dimensional Ising model, J. Phys. A: Math. Gen. **35**, 4861 (2002).

[48] R. H. Swendsen and J.-S. Wang, Nonuniversal critical dynamics in Monte Carlo simulations, Phys. Rev. Lett. **58**, 86 (1987).

[49] F. Belletti *et al.* (Janus Collaboration), Nonequilibrium spin-glass dynamics from picoseconds to one tenth of a second, Phys. Rev. Lett. **101**, 157201 (2008).

[50] L. A. Fernandez, E. Marinari, V. Martin-Mayor, I. Paga, and J. J. Ruiz-Lorenzo, Dimensional crossover in the aging dynamics of spin glasses in a film geometry, Phys. Rev. B **100**, 184412 (2019).

[51] D. J. Amit and V. Martín-Mayor, *Field Theory, the Renormalization Group and Critical Phenomena*, 3rd ed. (World Scientific, Singapore, 2005).

[52] L. A. Fernández and V. Martín-Mayor, Testing statics-dynamics equivalence at the spin-glass transition in three dimensions, Phys. Rev. B **91**, 174202 (2015).

[53] Y. Ozeki and N. Ito, Nonequilibrium relaxation method, J. Phys. A: Math. Theor. **40**, R149 (2007).

[54] H. Shao, W. Guo, and A. W. Sandvik, Quantum criticality with two length scales, Science **352**, 213 (2016).

[55] B. Nienhuis, Analytical calculation of two leading exponents of the dilute Potts model, J. Phys. A: Math. Gen. **15**, 199 (1982).

[56] A. E. Ferdinand and M. E. Fisher, Bounded and inhomogeneous Ising models. I. specific-heat anomaly of a finite lattice, Phys. Rev. **185**, 832 (1969).

[57] M. Bernaschi, I. González-Adalid Pemartín, V. Martín-Mayor, and G. Parisi, The QISG suite: High-performance codes for studying quantum Ising spin glasses, Comput. Phys. Commun. **298**, 109101 (2024).

[58] L. Chen, P. Jentsch, C. F. Lee, A. Maitra, S. Ramaswamy, and J. Toner, The inconvenient truth about flocks, arXiv:2503.17064.